

福昕PDF编辑器

• 永久 • 轻巧 • 自由

[点击升级会员](#)

[点击批量购买](#)



永久使用

无限制使用次数



极速轻巧

超低资源占用，告别卡顿慢



自由编辑

享受Word一样的编辑自由



扫一扫，关注公众号



Multiscale patch-based contrast measure for small infrared target detection



Yantao Wei^{a,b}, Xinge You^{a,*}, Hong Li^c

^a School of Electronic Information and Communications, Huazhong University of Science and Technology, Wuhan 430074, China

^b School of Educational Information Technology, Central China Normal University, Wuhan 430079, China

^c School of Mathematics and Statistics, Huazhong University of Science and Technology, Wuhan 430074, China

ARTICLE INFO

Article history:

Received 10 November 2015

Received in revised form

8 March 2016

Accepted 4 April 2016

Available online 14 April 2016

Keywords:

Local contrast

Small IR target detection

Image patch

Target enhancement

ABSTRACT

Infrared (IR) small target detection plays an important role in IR guidance systems. In this paper, a biologically inspired method called multiscale patch-based contrast measure (MPCM) is proposed for small IR target detection. MPCM can increase the contrast between target and background, which makes it easy to segment small target by simple adaptive thresholding method. Experimental results on three sequences demonstrate that the proposed small target detection method can not only suppress background clutter effectively even if with strong noise interference, but also detect targets accurately with low false alarm rate and high speed.

© 2016 Published by Elsevier Ltd.

1. Introduction

Small infrared (IR) target detection is one of the most important techniques in passive defense systems [1–5]. On the one hand, small targets are usually submerged in background clutter and heavy noise. On the other hand, the small targets do not have concrete shapes and textures, so there is no obvious feature and useful texture information can be used. Hence the small IR target detection is an extremely challenging task [6,7].

A lot of small IR target detection methods have been designed over the last two decades [8–11]. Existing methods focus mostly on how to “pop out” (enhance) the target and “neglect” (suppress) background regions as much as possible [12,8]. Existing techniques could be divided into two categories: detection based on single frame [13] and sequential frames, respectively [14]. The sequential detection methods need more prior information and usually based on the single frame detection. Consequently, sequential detection methods have limitation in military applications [14]. The detection based on single frame is of great importance due to the nature of early-warning [15]. A lot of conventional methods have been used in single frame detection [15], such as Top-hat filter [16], max-mean/max-median filter [17], high-pass filter, matched filter, and wavelet transformation [18,19]. However, these methods would result in serious false alarms and degraded

detection performance when the signal-clutter ratio (SCR) is low. In the small target detection, the edges of the targets can be used [20–22]. For instance, Laplacian of Gaussian (LoG) filters [23], an edge detector, has been used to detect small targets [24,20]. Targets can be enhanced and clutters can be suppressed significantly by LoG. However, the edge around cloud clutter can generate false detections, and the horizontal edge line due to a heterogeneous background produces false detections [25]. Recently, sparse representation [26] has been used for small target detection. Zhao et al. proposed sparse representation-based method for small target detection [27]. But it cannot describe the background very well. Zhao et al. then proposed the principal curvature-based method for small target detection [28]. However, this approach is not suitable for very dim and small targets.

Recently, a new trend towards imitating robust human visual system (HVS) for promoting the performance of small IR target detection has been emerging [20,1,29]. HVS-based methods have shown great potential in various target detection tasks, however, they still need to be improved. For example, Wang et al. developed an efficient method called average gray absolute difference maximum map (AGADMM) for multiscale small target detection [30]. But it roughly characterizes the background. Kim et al. proposed a HVS contrast mechanism-based detection algorithm, which is capable of increasing target intensity as well as suppressing background clutter and noise [20]. However, this method need to detect sea-sky line. In order to deal with this problem, we proposed a small IR target detection method called local contrast measure (LCM) [1]. However it assumes that the targets are brighter than the background. Subsequently, Han et al. proposed the improved

* Corresponding author.

E-mail addresses: yantaowei@mail.ccnu.edu.cn (Y.-A. Wei), yougx@mail.hust.edu.cn (X. You), hongli@mail.hust.edu.cn (H. Li).

LCM (ILCM) to improve detection rate and reduce false alarm rate, where the HVS size-adaptation process and attention shift mechanism are adopted [31]. But it smooths the targets. Shao et al. proposed an improved algorithm based on the contrast mechanism of HVS, which exploits LoG filter to deal with input image and processes the filtered image with morphological method in all directions [15]. A novel method called accumulated center-surround difference measure (ACSDM) was also proposed to detect small IR targets in heavy clutter [32]. But this method is very time-consuming.

The current research shows that defining the contrast between the target and background is one of the most important tasks in small IR target detection [33]. Consequently, a new local contrast measure method is defined in this paper from the perspective of image patch difference. Experimental results demonstrate that the proposed method has better detection performance comparing with several widely used methods. The contributions of this paper can be summarized as follows.

- An effective local contrast measure method called multiscale patch-based contrast measure (MPCM) is presented. The roles of the MPCM are twofold: the target of interest is enhanced, while complicated clutter and noise is adaptively suppressed. It can enhance the dark and bright targets simultaneously.
- Based on MPCM, a small IR target detection algorithm is designed. Experimental results show that the proposed method is effective with respect to detection accuracy, and faster than other methods.

This paper is organized as follows. Related work is given in Section 2. Section 3 provides a detailed description of the proposed MPCM. Based on MPCM, a new small IR target detection method is presented in Section 4. Although the proposed detection method is simple, it can achieve better performance. Section 5 presents the experimental results on three IR image sequences to demonstrate the effectiveness of the proposed target detection method. Finally, the conclusions and future works are provided in Section 6.



Fig. 1. The nested structure.

2. Related work

The concept of local contrast has been widely used in pattern recognition community [34,35]. Chen et al. proposed an effective measure called LCM for small target detection [1]. In LCM, a sliding window moves on the IR image from up to down and left to right pixel by pixel. Then the sliding window can be divided into 9 (3×3) subwindows. Note that the central subwindow denoted by "0" is a region where the target could appear. The gray mean of the i th subwindow is denoted by m_i ($i = 1, 2, \dots, 8$), that is,

$$m_i = \frac{1}{N_u} \sum_{j=1}^{N_u} l_j^i, \quad (1)$$

where N_u is the number of the pixels in the i th subwindow, and l_j^i is the gray level of the j th pixel in the i th subwindow. Hence, the contrast between central subwindow and the i th surrounding subwindow is defined by

$$c_i = \frac{L_0}{m_i}, \quad (2)$$

where L_0 represents the maximum of the gray value of the central subwindow.

In IR image, target is usually brighter than that of their neighborhoods. So the LCM is defined as follows:

$$C = \min_i L_0 \times c_i = \min_i L_0 \times \frac{L_0}{m_i} = \min_i \frac{L_0^2}{m_i}. \quad (3)$$

This definition means that the larger the C is, the more likely a target appears. If $(L_0/m_i) = (L_0'/m_i')$, then the larger of L_0 and L_0' is more likely to correspond to a target.

In fact, the sizes of small targets are changing. In the ideal case, the size of subwindow should be the same as the target size. In order to deal with this problem, multiscale LCM has been defined. Sequentely the ILCM is proposed to pursuit a good performance in the detection rate, false alarm rate, and speed simultaneously [36]. The proposed MPCM is an improved version of the LCM too.

3. Multiscale patch-based contrast measure

In human visual streams, contrast is one of the most important quantities [20]. Using this mechanism, we can perceive the world similarly regardless of the huge changes in illumination over the day or from place to place. On the other hand, IR target has the signature of discontinuity comparing with its neighborhood but no obvious structural information [1,31]. For these reasons, designing effective target enhancement method based on contrast mechanism is a possible way to promote the performance of the small target detection system. In this paper, a small IR target enhancement method inspired by the contrast mechanism of HSV is proposed. Firstly, local contrast of each pixel is computed by the defined patch difference on each scale, then the final contrast map consisting of each pixel's MPCM is obtained by taking the

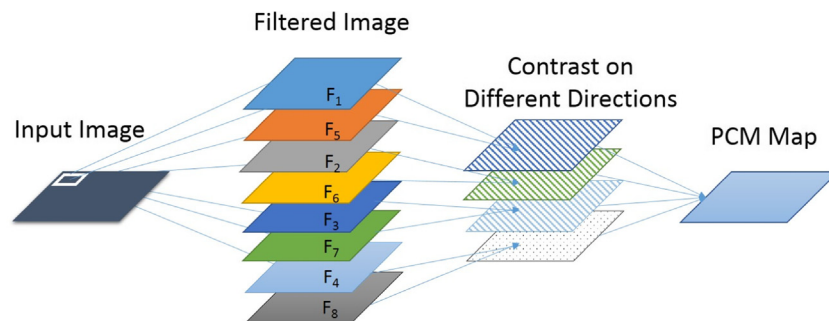


Fig. 2. The flowchart of PCM.

maximum value between different scales. In the final contrast map, the MPCM of a pixel means the probability of it belonging to the target region.

3.1. Computation of patch-based contrast measure

In order to give the definition of the proposed measure, a nested structure is given in Fig. 1. Firstly, a sliding window is divided into two parts, where the central part denoted by T (Fig. 1) is the reference patch (targets may appear), and the surrounding part is the background. In order to measure the local contrast more precisely, we divided the surrounding part into 8 patches $B_i, i = 1, 2, \dots, 8$. The proposed measure aims at enhancing the target and suppressing the background. So the definition of the proposed method can be given as follows.

The dissimilarity between reference patch T and background patch B_i can be defined by

$$D(T) = \begin{pmatrix} d(T, B1) \\ d(T, B2) \\ \vdots \\ d(T, B8) \end{pmatrix}, \quad (4)$$

where d is a dissimilarity measure. Currently, there are many dissimilarity measure methods. In this paper, the d is defined by

$$d(T, Bi) = m_T - m_{Bi}, \quad (i = 1, 2, \dots, 8) \quad (5)$$

where m_T and m_{Bi} are the means of the central patch and the i th background patch, respectively.

Based on the previous preparation, a local contrast measure on a certain scale can be given. For a small target, there is grayscale intensity difference between target area and its surrounding background. That is to say the intensity of the target is higher or smaller than that of the background patches. In order to characterize this property, we give the definition as

$$\tilde{d}_i = d(T, Bi) * d(T, Bi+4), \quad (i = 1, 2, \dots, 4). \quad (6)$$

\tilde{d}_i measures the dissimilarity between the reference patch and the background patches on the i th direction. We can also find that $\tilde{d}_i > 0$ when $d(T, Bi)$ and $d(T, Bi+4)$ have the same signs. This means that the intensity of the reference patch is higher or smaller than that of background patches. Consequently, (6) is consistent with the characteristic of the target region.

In small target enhancement, the contrast between the target region and background region should be as large as possible. For this reason, the minimum distance between the reference patch and its surrounding background patches can be taken as a measure of contrast. So we can compute the patch-based contrast measure (PCM) on a given scale in the following way:

$$C_{(x_{ii}, y_{jj})} = \min_{i=1,2,3,\dots,4} \tilde{d}_i, \quad (7)$$

where (x_{ii}, y_{jj}) is the coordinate of the central pixel in reference patch T . The computation process of PCM is given in Algorithm 1, where N is the width and height of the image patch, $\text{floor}(N/2)$ rounds $N/2$ to the nearest integer less than or equal to $N/2$. In this way, we can obtain a contrast map C at a given scale. It is easy to find that the proposed method is simple.

Algorithm 1. Computing PCM.

Input: Require Input Image.

Output: C .

1: Compute the mean of T according to

$$m_T = \frac{1}{N \times N} \sum_{i=x_{ii}-\text{floor}(N/2)}^{x_{ii}+\text{floor}(N/2)} \sum_{j=y_{ii}-\text{floor}(N/2)}^{y_{ii}+\text{floor}(N/2)} f(x_i, y_j) \quad (8)$$

2: Compute, B_i , the mean of each background patch.

3: Obtain $C_{(x_{ii}, y_{jj})}$ according to (7).

4: if the sliding window has scanned the whole image then

5: Output C .

6: else

7: Moving the sliding window to the next position.

8: Repeat steps 1–7 to compute the PCM of the new position.

9: end if

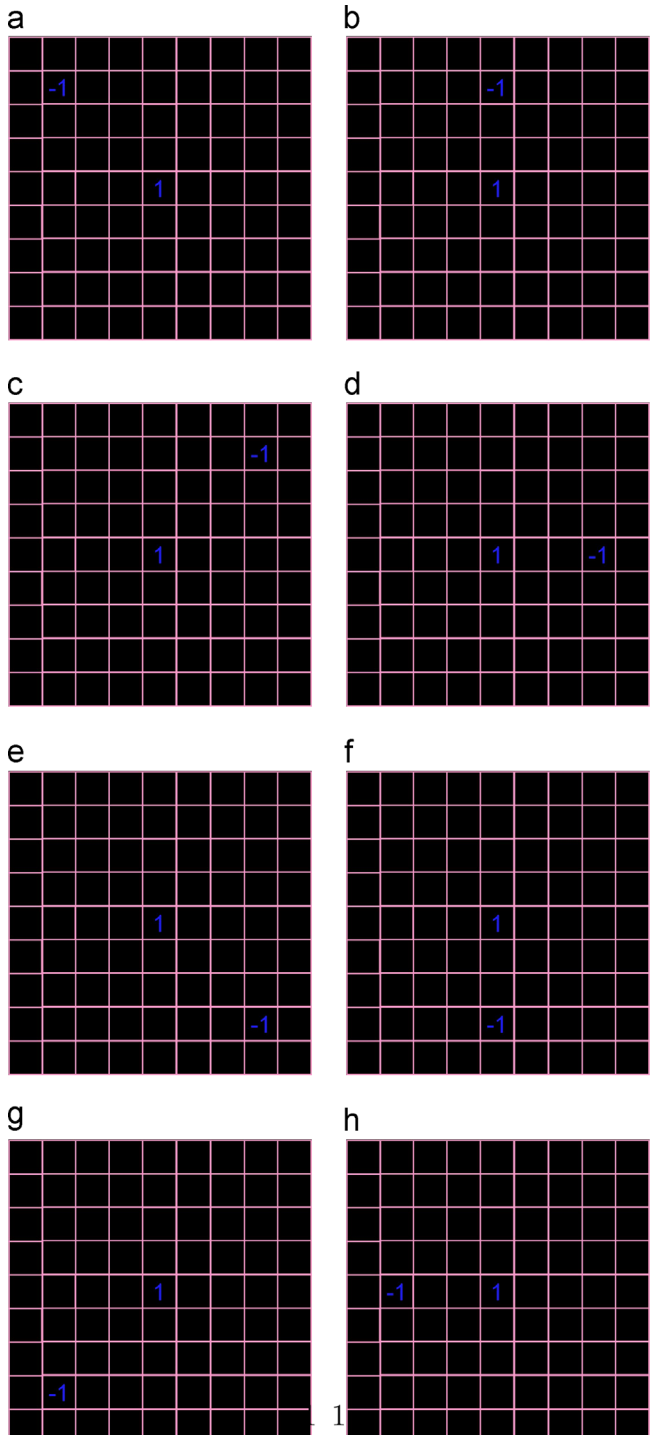


Fig. 3. All of the filters. (a) Filter 1; (b) Filter 2; (c) Filter 3; (d) Filter 4; (e) Filter 5; (f) Filter 6; (g) Filter 7; (h) Filter 8.

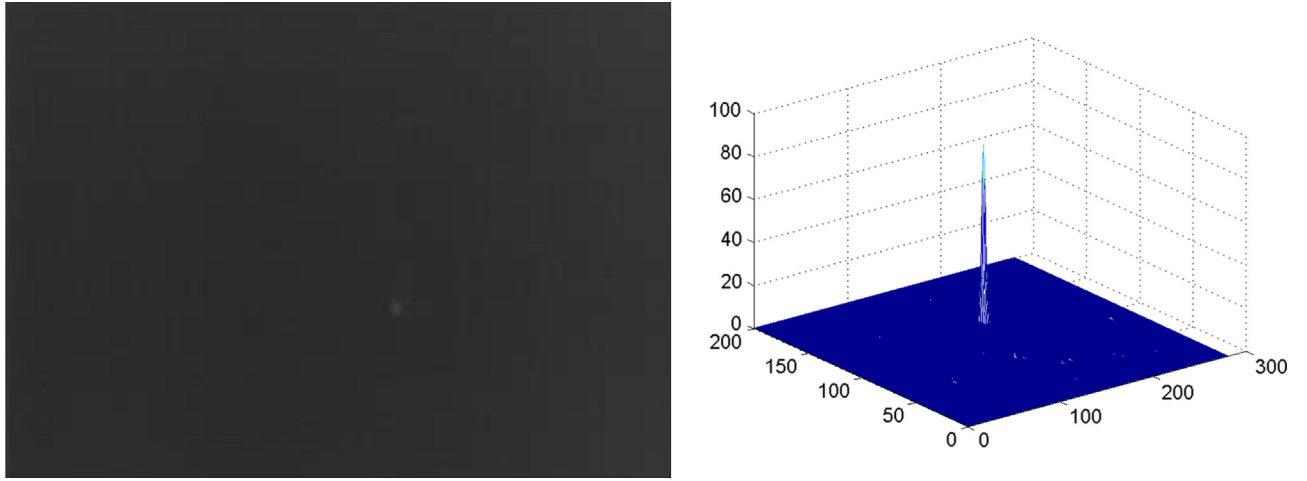


Fig. 4. Example of the MPCM. (a) Original IR image, (b) 3D mesh view of the MPCM map.

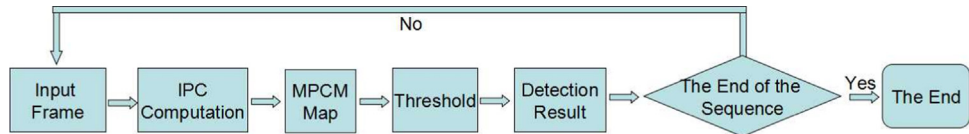


Fig. 5. The flowchart of MPCM-based small target detection method.

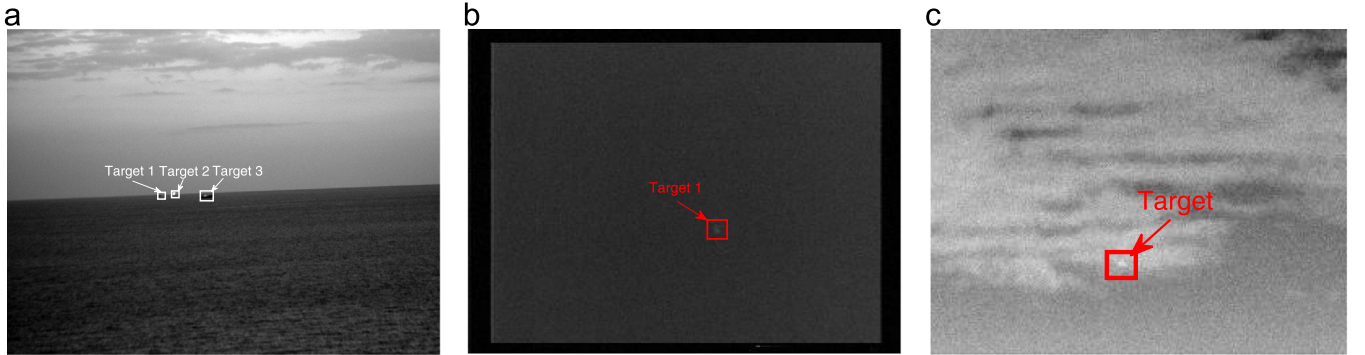


Fig. 6. The original images. (a) Image belonging to M sequence; (b) image belonging to P sequence; (c) image belonging to S sequence.

In practice, the local contrast on a given scale can be obtained by the filtering operations. Consequently, the procedure given in [Algorithm 1](#) can be rewritten as (see [Fig. 2](#)):

- Firstly, the given frame can be filtered by a mean filter. The size of the filter is $N \times N$.
- Secondly, the filtered image can be filtered by 8 filters given in [Fig. 3](#), where $N=3$. The filters shown in [Fig. 3](#) are designed for computing the local differences on different directions (8 directions), where there are 79 zeros in each filter. For example, [Fig. 3\(a\)](#) shows the filter computing the $d(T, B1)$. This is convenient to the implementation of MPCM. The output maps are denoted by F_i ($i = 1, 2, \dots, 8$).
- Thirdly, dot product operation is carried out on the output maps according to Eq. (6).
- Finally, obtain the PCM according to Eq. (7).

3.2. Multiscale patch-based contrast measure

In practice, the size of small target cannot be determined previously. The window's size should be approximated to the size of the

Table 1
Comparison of several target detection methods on sequence M.

Method	Top-hat	AGADMM	ACSDM	LCM	ILCM	Proposed
P_d	66.67	100.0	100.0	66.67	33.33	100.0
P_f	0.000	0.000	0.000	0.000	0.000	0.000
Time (s)	0.930	1.162	7.742	9.239	2.293	0.468

small target. Consequently, MPCM is given in [Algorithm 2](#), where \hat{C} is the MPCM map, C^l is the PCM map on the l th scale, L is the maximum scale, p_1 and q_1 are the numbers of rows and columns of the contrast map, respectively. [Fig. 4](#) shows one example of the MPCM. It indicates that the proposed method can enhance small dim targets. And the experimental results also show that MPCM can resolve the problem of edge response encountered by the LoG filter [20].

Algorithm 2. Multiscale PCM.

Input: Input Image

Output \hat{C}

1: **for** $l = 1 : L$ **do**

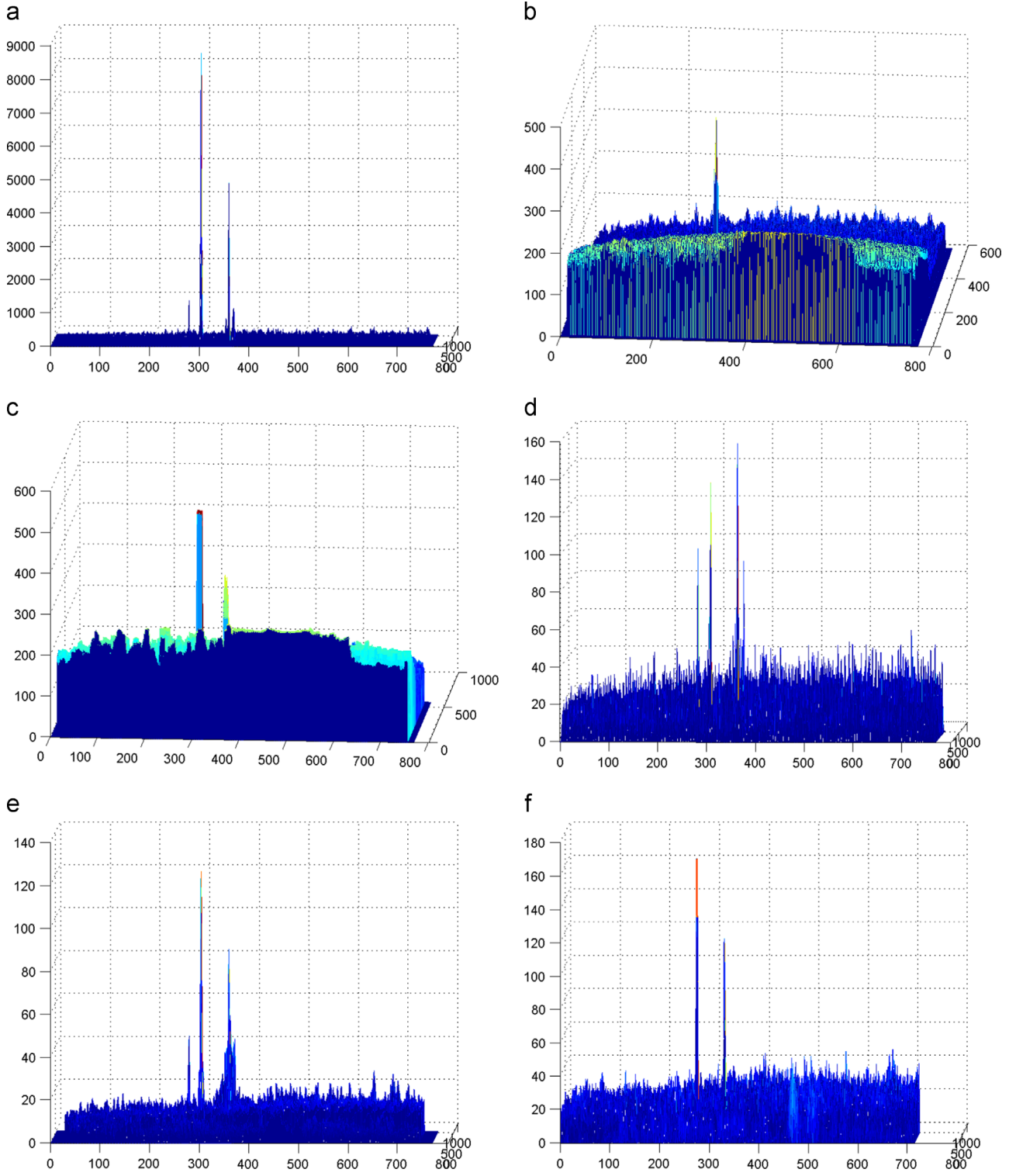


Fig. 7. Enhanced images of different methods on sequence M. (a) Result of the proposed method; (b) result of ILCM; (c) result of LCM ; (d) result of ACSDM; (e) result of AGADMM; (f) result of Top-hat.

```

2: Compute the contrast map,  $\mathcal{C}^l$ , according to Algorithm 1.
3: end for
4: for  $p = 1 : p_1$  do
5:   for  $q = 1 : q_1$  do

```

$$\hat{c}_{p,q} = \max_{l=1,2,\dots,L} \mathcal{C}^l(p,q)$$

```

6:   end for
7: end for

```

In MPCM, the width of the patch, N , is a key parameter. If N is too small, the potential target may be masked by background. On the other hand, if N is too large, the operation will consume more

computation. The small target in IR image often occupies several pixels, the appropriate patch size should be no more than 81 pixels [1]. The classification includes point source targets, small extended targets, clusters of point source targets and small extended targets [1]. Correspondingly, N is not larger than 9 in the experiments.

4. The proposed small target detection method

4.1. Small target detection method based on MPCM

According to the definition of MPCM, the local contrast measure of each frame can be obtained. Once the MPCM map is computed, then the targets can be segmented by an adaptive thresholding method. Here, the threshold τ is determined by [1]

$$\tau = \mu + K\delta, \quad (9)$$

where k is a parameter,

$$\mu = \frac{1}{p_1 q_1} \sum_{i=1}^{p_1} \sum_{j=1}^{q_1} \hat{C}_{ij} \quad (10)$$

is the mean of \hat{C} , and

$$\delta = \sqrt{\frac{1}{p_1 q_1} \sum_{i=1}^{p_1} \sum_{j=1}^{q_1} (\hat{C}_{ij} - \mu)^2} \quad (11)$$

is the standard deviation of \hat{C} . The threshold is various in different tasks because the size of target, IR imaging device, and weather affect the determination of the threshold [28]. Consequently, K is assigned by experience. In our experiments, K ranges from 3 to 14 (see Section 5). The flowchart of the proposed detection method is given in Fig. 5. In summary, the proposed method consists of two stages: target enhancement and adaptive threshold segmentation. In the first stage, the target is enhanced and the background clutter is suppressed. In the second stage, a suitable threshold is obtained by (9). The experimental results show that the threshold can be chosen from a wide dynamic range.

4.2. Discussion

From the definition of MPCM, we can find that it is simple and fit for parallel computing. Eq. (5) shows that if all $d(T, Bi) > 0$ in the target region, then T is a bright target, otherwise T is a dark target. According to this property, MPCM has two special cases. If there are only bright targets (the fighter in the sky) in a known application scenario, then (6) can be rewritten as

$$\tilde{d}_i = \begin{cases} d(T, Bi) * d(T, Bi+4) & \text{if } d(T, Bi) > 0 \text{ and } d(T, Bi+4) > 0 \\ 0 & \text{otherwise,} \end{cases} \quad (12)$$

where $i = 1, 2, \dots, 4$. Similarly, if the target is darker than the background, then

$$\tilde{d}_i = \begin{cases} d(T, Bi) * d(T, Bi+4) & \text{if } d(T, Bi) < 0 \text{ and } d(T, Bi+4) < 0 \\ 0 & \text{otherwise.} \end{cases} \quad (13)$$

The MPCM based on (6) can simultaneously enhance the bright

and dark targets. While MPCM based on (12) and (13) can enhance the bright and dark targets, respectively. Consequently, the proposed method is more flexible and has wide application prospects.

Next, we will give theoretical analysis of the MPCM. This will help us understand why the proposed method is effective. First, as mentioned in Section 3.1, the mean filtering can be carried out firstly in the computation of MPCM. Consequently, the clutter and noise can be suppressed by this operation.

Second, the MPCM can enhance the target and suppress the background. Without loss of generality, we assume the target is brighter than the background. When $d(T, Bi)$ and $d(T, Bi+4)$ have different signs, a smaller contrast will be obtained. And when $d(T, Bi)$ and $d(T, Bi+4)$ have the same signs, we have

$$C_{(x_i, y_j)} = \min_{i=1,2,3,4} \tilde{d}_i = \min_{i=1,2,3,4} d(T, Bi) * d(T, Bi+4) \geq d(T, Bi)^2 = (T - m_i)^2 \quad (14)$$

where m_i is the largest means of the surrounding patches.

Let

$$f(T) = (T - m_i)^2, \quad (15)$$

then we have

$$f'(T) = 2(T - m_i). \quad (16)$$

Eq. (16) shows that the larger T leads to larger $f(T)$. This means that when T is the target, the contrast value will increase significantly. Conversely, when T is the background, it is similar to one of its surrounding patches. In this case, the contrast approaches zero. Consequently, we can find that the proposed method can enhance the target and suppress the background.

5. Experimental results and analysis

To demonstrate the effectiveness of the proposed method, three real IR image sequences with various heavy clutters, denoted by M, P, and S, are used. Note that sequences P and S are corrupted by noise. Example images are shown in Fig. 6.

To compare the performance of different methods quantitatively, we use the detection probability P_d defined in (17) and probability of false alarm P_f defined in (18). The P_d is calculated as the number ratio of correctly detected targets to totally real targets, and the P_f is calculated as the number ratio of incorrectly detected targets to totally detected targets.

$$P_d = \frac{\text{The number of correctly detected targets}}{\text{The number of totally real targets}} \times 100\% \quad (17)$$

and

$$P_f = \frac{\text{The number of incorrectly detected targets}}{\text{The number of totally detected targets}} \times 100\%. \quad (18)$$

If the distance between a ground truth and a detected position is within a threshold (5 pixels), then the detection is declared as being correct [20]. And if the percentage of overlapping area between detected target and ground truth target is larger than 50%, then detected target will be taken as the correct detection. In addition, the time consumed by different methods are also given. In this paper, Top-hat, AGADMM, ACSDM, LCM and ILCM are used to compare the performance of IR small target detection. The Top-hat is a baseline method, and is widely used in the literatures. AGADMM and ACSDM are based on local difference, and they have something in common with the proposed method. For the proposed method, we have $L=3$, and $N=3, 5, 7$. All experiments are carried out using MATLAB on an Intel i7 quadcore 2.10-GHz machine with 8 GB RAM.

Table 2
Comparison of several target detection methods on sequence P.

Method	Top-hat	AGADMM	ACSDM	LCM	ILCM	Proposed
P_d	66.67	93.33	41.67	86.67	65.00	98.33
P_f	38.46	24.32	33.78	13.33	22.00	7.81
Time (s)	0.6674	0.6010	1.5080	1.378	1.918	0.4883

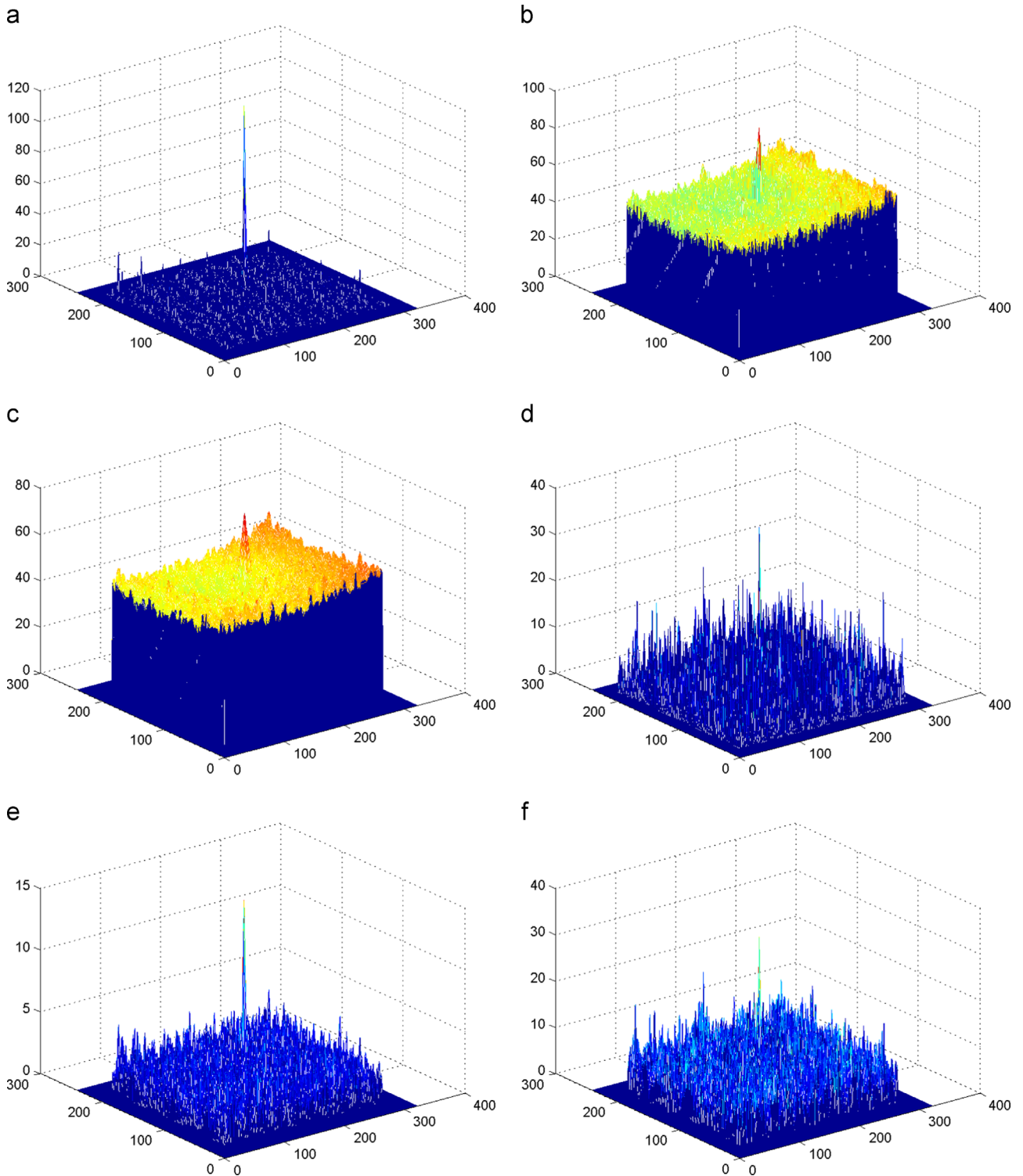


Fig. 8. Enhanced images of different methods on sequence P. (a) Result of the proposed method; (b) result of ILCM; (c) result of LCM ; (d) result of ACSDM; (e) result of AGADMM; (f) result of Top-hat.

Table 3
Comparison of several target detection methods on sequence S.

Method	Top-hat	AGADMM	ACSDM	LCM	ILCM	Proposed
P_d	92.86	98.57	90.00	100	91.43	100
P_f	10.96	12.66	20.25	2.778	4.478	0.000
Time (s)	0.400	0.3733	1.119	1.087	0.7109	0.2863

5.1. Experiments on sequence M

As shown in Fig. 6, there are three small targets (ships) in sequence M. They are different from each other. The size of the image is 576×768 pixels. We also find that the targets in Fig. 6 (a) are not always brighter than the background. So the methods assuming that the targets in the IR image have larger intensity do

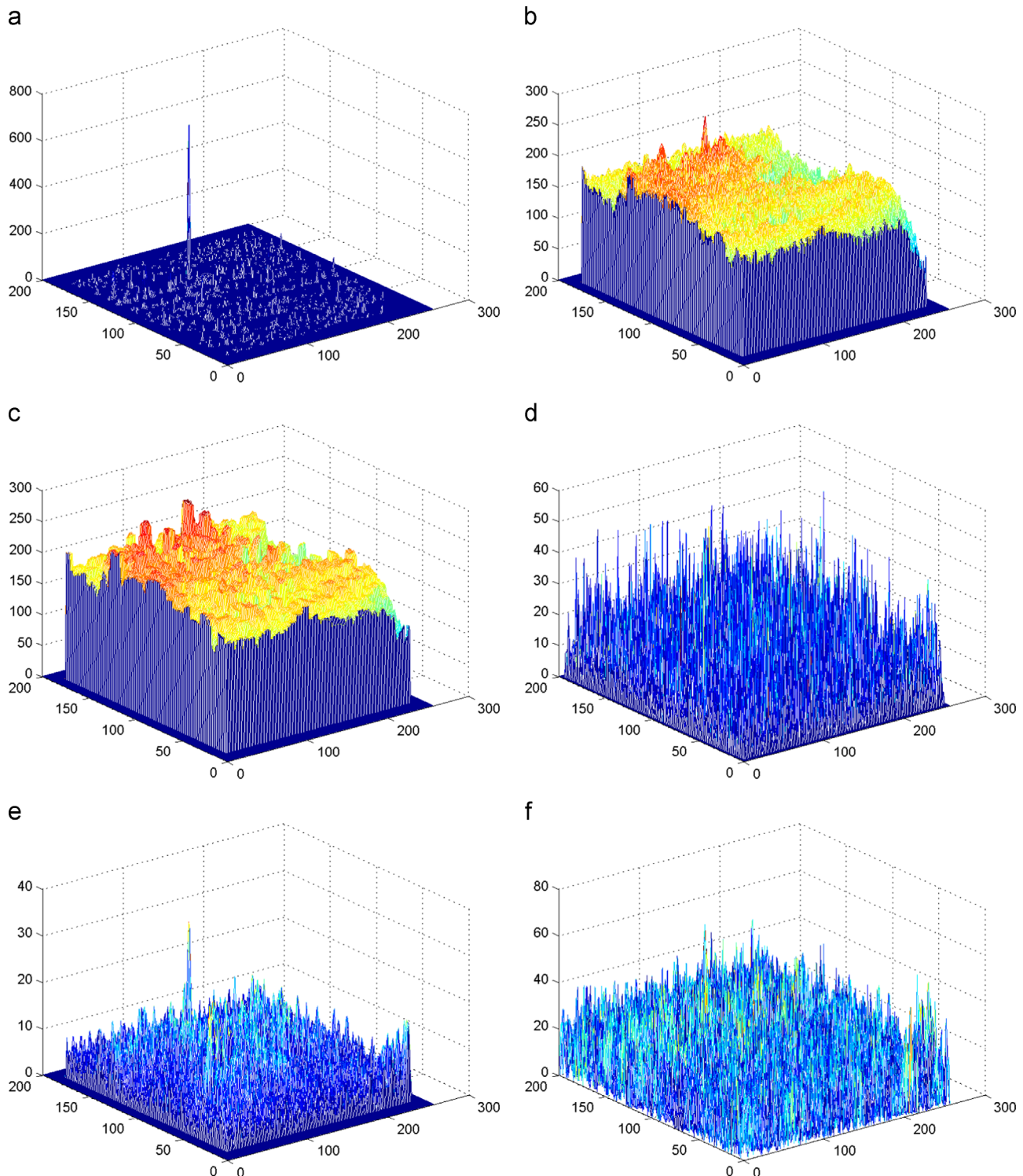


Fig. 9. Enhanced images of different methods on sequence S. (a) Result of the proposed method; (b) result of ILCM; (c) result of LCM; (d) result of ACSDM; (e) result of AGADMM; (f) result of Top-hat.

Table 4

Comparison of several target detection methods on sequence M with salt and pepper noise.

Method	Top-hat	AGADMM	ACSDM	LCM	ILCM	Proposed
P_d	66.67	100.0	33.33	66.67	33.33	100.0
P_f	80.58	16.67	93.49	82.30	16.67	3.226

Table 5

Comparison of several target detection methods on sequence M with Gaussian noise.

Method	Top-hat	AGADMM	ACSDM	LCM	ILCM	Proposed
P_d	66.67	100.0	90.00	66.67	33.33	100.0
P_f	4.762	0.000	6.897	0.000	0.000	0.000

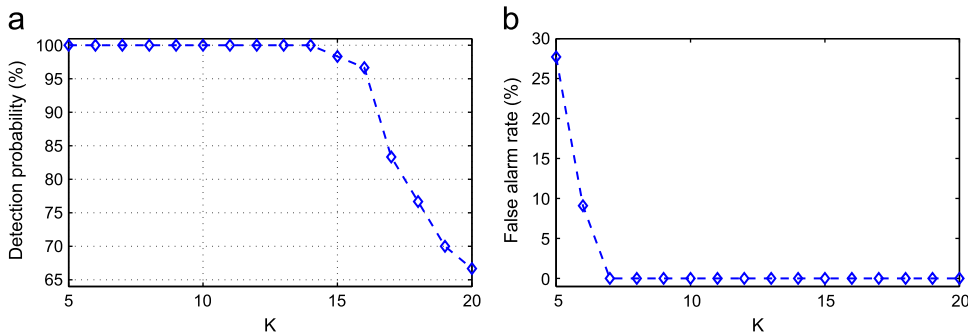


Fig. 10. Effect of different K 's on M sequence. (a) Detection probabilities; (b) false alarm rates.

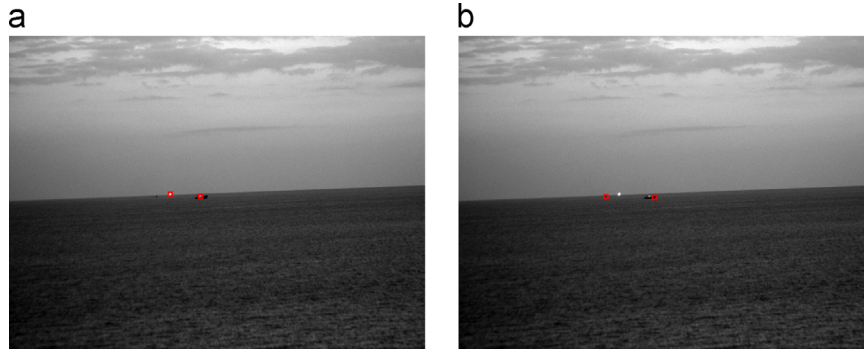


Fig. 11. Detection result of different methods. (a) Detection result obtained by Eq. (12); (b) detection result obtained by Eq. (13).

not work well. Due to the long distance, the dark target appears as a weak dim point embedded in the complex background. Consequently, it is too difficult to be detected. This sequence has 20 frames. The detection results of different methods are given in Table 1. In this experiment, K equals 7. We find that our method can detect the bright and dark targets simultaneously. The experimental results also show that the proposed method is fast. Table 1 show that although ILCM is faster than LCM, it is not fully competent in dim and small target detection because it miss the interesting target.

Furthermore, the 3D mesh view of the enhanced images corresponding to different methods are given in Fig. 7. We can observe that the targets are enhanced significantly and the background clutter is suppressed by our method. This also indicates that our method can improve the SCR of the input image significantly, and is not sensitive to sea-sky line of the IR image. The reason for this is that the output of Eq. (7) is very small, if the reference patch is on the sea-sky line. In addition, we find that LCM and ILCM cannot enhance dark targets.

5.2. Experiments on sequence P

For original sequence P, the imaging sensor, located at a distance of about 15–25 km from the target, was on ground searching the aircraft in sky. The operating wavelength of the IR camera is $8.3\text{ }\mu\text{m}$ and its resolution is 320×240 pixels. This sequence was captured on a sunny day [1]. As shown in Fig. 6(b), a small target is embedded in the complex background. There are 60 frames can be used to verify the effectiveness of the proposed method. This sequence has a low SCR. So it is difficult to detect and track the target in this sequence.

Table 2 shows the P_d 's, P_f 's and computation time of different methods, where $K=13$. These experimental results indicate that our method outperforms other methods in its significant

increment of P_d and reduction of P_f 's. The detection experiment results also illustrate that the proposed method is very fast. Furthermore, 3D mesh view of the enhanced images are given in Fig. 8. The effectiveness of our method can be visually verified. It is easy to see that the proposed method gives impressive results. These results also show that our method is robust to noise. The reason for this maybe that mean filtering operation is carried out on the input image. Consequently, the proposed method can detect the targets efficiently.

5.3. Experiments on sequence S

Finally, we evaluate the performance of the proposed method on the sequence S. In this sequence, the target is a fighter, and the resolution is 256×200 pixels. There are 70 frames in this sequence. As can be seen from Table 3, our method has the best performance. Fig. 9 shows that the proposed method can enhance the target and suppress the background clutter significantly, where $K=12$. ACSDM and Top-hat are sensitive to noise. For Top-hat and ACSDM, it is difficult to find a suitable threshold to segment the targets on this sequence. Although AGADMM can detect the targets with higher P_d , it has higher P_f .

5.4. Discussion

In order to further analyze the proposed method, we test its performance on more experiments. The experimental results on the M sequence are reported and the same conclusions can be made on the other sequences.

Firstly, in order to demonstrate the robustness of the proposed method, it was tested on the image sequence corrupted with known noise. In this experiment, salt and pepper noise of density 0.00005 is added to each frame. The experimental results are given in Table 4. These results show that the proposed method

achieves low P_f and high P_d . In addition, Gaussian white noise of variance 0.001 is added to each frame. Table 5 shows the experimental results. The proposed method performs the best. We can find that the proposed method is more robust to noise.

Secondly, we show effects of the K on the detection performance. We perform the small target detection with different K 's, and the P_d 's and P_f 's are given in Fig. 10. The experimental results show that the proposed method performs the best when $K \in [7 \text{--} 14]$. This shows that K has wide dynamic range, and helps us to determine K to obtain higher classification accuracy. In our experiments on three image sequences, all the best performances was obtained when K belongs to this range.

Finally, we verified the effectiveness of Eqs. (12) and (13). Fig. 11 shows the detection results. In this sequence, there are three targets, one is bright, another is dark, and the other is hybrid. We can find that Eqs. (12) and (13) can detect bright and dark targets, respectively. In addition, we also find that Eqs. (12) and (13) can suppress more background clutter.

6. Conclusions

This paper presents an effective method for small IR target detection based on the patch contrast. The main idea is to define the local contrast measure based on patch differences for suppressing the background and enhancing the targets. We note that the computation speed can be accelerated by parallel computations. It can be easily carried out by GPU [37]. The effectiveness of the proposed method has been demonstrated on three different detection scenarios. Experimental results have verified that our method can efficiently detect targets with different types of backgrounds. We can conclude that our method is fast and obtain higher detection accuracy. Consequently, it is fit for small IR target detection. However, the choosing of threshold is still a challenge. It will be studied in the future. In addition, only first order information is used in our method. Consequently, the higher order information will be considered in our future work.

Conflict of interest

None declared.

Acknowledgments

This work was supported in part by National Natural Science Foundation of China under Grants 61502195, 61472155, 61571205 and 61272203, the International Scientific and Technological Cooperation Program of China under Grant 2011DFA12180, the Hubei Province Science and Technology Support Program under Grant 2013BAA120, the Shenzhen Research Council under Grant JCYJ20140819154343378, and by the Fundamental Research Funds for the Central Universities under Grants CCNU14A05023 and CCNU16A05022.

References

- [1] C.P. Chen, H. Li, Y. Wei, T. Xia, Y.Y. Tang, A local contrast method for small infrared target detection, *IEEE Trans. Geosci. Remote Sens.* 52 (1) (2014) 574–581.
- [2] B. Du, L. Zhang, Target detection based on a dynamic subspace, *Pattern Recognit.* 47 (1) (2014) 344–358.
- [3] C. Yang, J. Ma, S. Qi, J. Tian, S. Zheng, X. Tian, Directional support value of gaussian transformation for infrared small target detection, *Appl. Opt.* 54 (9) (2015) 2255–2265.
- [4] H. Li, Y. Tan, Y. Li, J. Tian, Image layering based small infrared target detection method, *Electron. Lett.* 50 (1) (2014) 42–44.
- [5] A. Dehghani, A. Pourmohammad, Small target detection and tracking based on the background elimination and kalman filter, in: 2015 International Symposium on Artificial Intelligence and Signal Processing (AISP), IEEE, Mashhad, Iran, 2015, pp. 328–333.
- [6] H. Qi, B. Mo, F. Liu, Y. He, S. Liu, Small infrared target detection utilizing local region similarity difference map, *Infrared Phys. Technol.* 71 (2015) 131–139.
- [7] J. Hu, Y. Yu, F. Liu, Small and dim target detection by background estimation, *Infrared Phys. Technol.* 73 (2015) 141–148.
- [8] S. Qi, D. Ming, J. Ma, X. Sun, J. Tian, Robust method for infrared small-target detection based on boolean map visual theory, *Appl. Opt.* 53 (18) (2014) 3929–3940.
- [9] C. Gao, D. Meng, Y. Yang, Y. Wang, X. Zhou, A.G. Hauptmann, Infrared patch-image model for small target detection in a single image, *IEEE Trans. Image Process.* 22 (12) (2013) 4996–5009.
- [10] C. Zheng, H. Li, Small infrared target detection based on harmonic and sparse matrix decomposition, *Opt. Eng.* 52 (6) (2013).
- [11] C. Gao, T. Zhang, Q. Li, Small infrared target detection using sparse ring representation, *IEEE Aerosp. Electron. Syst. Mag.* 27 (3) (2012) 21–30.
- [12] X. Bai, F. Zhou, T. Jin, Enhancement of dim small target through modified top-hat transformation under the condition of heavy clutter, *Signal Process.* 90 (5) (2010) 1643–1654.
- [13] H. Li, S. Xu, L. Li, Dim target detection and tracking based on empirical mode decomposition, *Signal Process.: Image Commun.* 23 (10) (2008) 788–797.
- [14] Y. He, M. Li, J. Zhang, Q. An, Small infrared target detection based on low-rank and sparse representation, *Infrared Phys. Technol.* 68 (2015) 98–109.
- [15] X. Shao, H. Fan, G. Lu, J. Xu, An improved infrared dim and small target detection algorithm based on the contrast mechanism of human visual system, *Infrared Phys. Technol.* 55 (5) (2012) 403–408.
- [16] X. Bai, F. Zhou, Analysis of new top-hat transformation and the application for infrared dim small target detection, *Pattern Recognit.* 43 (6) (2010) 2145–2156.
- [17] S. D. Deshpande, H. E. Meng, R. Venkateswarlu, P. Chan, Max-mean and max-median filters for detection of small targets, in: SPIE's International Symposium on Optical Science, Engineering, and Instrumentation, 1999, pp. 74–83.
- [18] L. Li, Y.Y. Tang, Wavelet-hough transform with applications in edge and target detections, *Int. J. Wavelets Multi-Resolut. Inf. Process.* 4 (3) (2006) 567–587.
- [19] K.N. Le, K.P. Dabke, G.K. Egan, Hyperbolic wavelet family, *Rev. Sci. Instrum.* 75 (11) (2004) 4678–4693.
- [20] S. Kim, J. Lee, Scale invariant small target detection by optimizing signal-to-clutter ratio in heterogeneous background for infrared search and track, *Pattern Recognit.* 45 (1) (2012) 393–406.
- [21] J.-W. Lu, Y.-J. He, H.-Y. Li, F.-L. Lu, Detecting small target of ship at sea by infrared image, in: IEEE International Conference on Automation Science and Engineering, 2006. CASE'06, IEEE, Shanghai, China, 2006, pp. 165–169.
- [22] K.N. Le, A mathematical approach to edge detection in hyperbolic-distributed and gaussian-distributed pixel-intensity images using hyperbolic and Gaussian masks, *Digital Signal Process.* 21 (1) (2011) 162–181.
- [23] Z. Miao, X. Jiang, Interest point detection using rank order log filter, *Pattern Recognit.* 46 (11) (2013) 2890–2901.
- [24] S. Kim, Min-local-log filter for detecting small targets in cluttered background, *Electron. Lett.* 47 (2) (2011) 105.
- [25] S. Kim, J. Lee, Small infrared target detection by region-adaptive clutter rejection for sea-based infrared search and track, *Sensors* 14 (7) (2014) 13210–13242.
- [26] W. Li, Q. Du, B. Zhang, Combined sparse and collaborative representation for hyperspectral target detection, *Pattern Recognit.* 48 (12) (2015) 3904–3916.
- [27] J. Zhao, Z. Tang, J. Yang, E. Liu, Infrared small target detection using sparse representation, *J. Syst. Eng. Electron.* 22 (6) (2011) 897–904.
- [28] Y. Zhao, H. Pan, C. Du, Y. Zheng, Principal curvature for infrared small target detection, *Infrared Phys. Technol.* 69 (2015) 36–43.
- [29] S. Qi, J. Ma, C. Tao, C. Yang, J. Tian, A robust directional saliency-based method for infrared small-target detection under various complex backgrounds, *IEEE Geosci. Remote Sens. Lett.* 10 (3) (2013) 495–499.
- [30] G. Wang, T. Zhang, L. Wei, N. Sang, Efficient method for multiscale small target detection from a natural scene, *Opt. Eng.* 35 (3) (1996) 761–768.
- [31] J. Han, Y. Ma, B. Zhou, F. Fan, K. Liang, Y. Fang, A robust infrared small target detection algorithm based on human visual system, *IEEE Geosci. Remote Sens. Lett.* 11 (12) (2014) 2168–2172.
- [32] K. Xie, K. Fu, T. Zhou, J. Zhang, J. Yang, Q. Wu, Small target detection based on accumulated center-surround difference measure, *Infrared Phys. Technol.* 67 (2014) 229–236.
- [33] C. Wang, S. Qin, Adaptive detection method of infrared small target based on target-background separation via robust principal component analysis, *Infrared Phys. Technol.* 69 (2015) 123–135.
- [34] W.-C. Kao, M.-C. Hsu, Y.-Y. Yang, Local contrast enhancement and adaptive feature extraction for illumination-invariant face recognition, *Pattern Recognit.* 43 (5) (2010) 1736–1747.
- [35] D. Gragnaniello, G. Poggi, C. Sansone, L. Verdoliva, Local contrast phase descriptor for fingerprint liveness detection, *Pattern Recognit.* 48 (4) (2015) 1050–1058.
- [36] J. Han, Y. Ma, B. Zhou, F. Fan, K. Liang, Y. Fang, A robust infrared small target detection algorithm based on human visual system, *IEEE Geosci. Remote Sens. Lett.* 12 (5) (2014) 2168–2172.
- [37] M. A. Javed, X. Guili, Y. Jie, N. Li, S. Y. Shah, GPU based small target detection using IR images, in: 2012 9th International Bhurban Conference on Applied Sciences and Technology (IBCAST), IEEE, Islamabad, Pakistan, 2012, pp. 92–94.

Yantao Wei received the B.Sc. degree in Information and Computing Science from the Qingdao University of Science and Technology, China, in 2006, the M.S. degree in Computational Mathematics from the Huazhong University of Science and Technology, China, in 2008 and the Ph.D. degree in Control Science and Engineering from Huazhong University of Science and Technology, China, in 2012. Currently, he is with the School of Electronic Information and Communications, Huazhong University of Science and Technology, and School of Educational Information Technology, Central China Normal University, China. His current research interests include computer vision and pattern recognition.

Xinge You received the B.S. and M.S. degrees in mathematics from the Hubei University, Wuhan, China, and the Ph.D. degree from the Department of Computer Science from the Hong Kong Baptist University, Hong Kong, in 1990, 2000, and 2004, respectively. Currently, he is a Professor at the School of Electronic Information and Communications in Huazhong University of Science and Technology, China. His current research interests include wavelets and its application, signal and image processing, pattern recognition, machine learning, and computer vision.

Hong Li received the M.Sc. degree in Mathematics and the Ph.D. degree in Pattern Recognition and Intelligence Control from the Huazhong University of Science and Technology, Wuhan, China, in 1986 and 1999, respectively. She is currently a Professor with the School of Mathematics and Statistics, Huazhong University of Science and Technology. Her current research interests include wavelet analysis, learning theory, and pattern recognition.